Marine and Petroleum Geology 138 (2022) 105550

Contents lists available at ScienceDirect

Marine and Petroleum Geology

journal homepage: www.elsevier.com/locate/marpetgeo

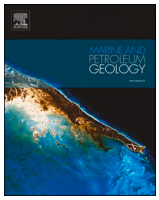

In-situ temperatures and thermal properties of the East Siberian Arctic shelf sediments: Key input for understanding the dynamics of subsea permafrost

E. Chuvilin [a,b,*], B. Bukhanov [a,b], A. Yurchenko [a], D. Davletshina [a], N. Shakhova [b,c], E. Spivak [b], V. Rusakov [d], O. Dudarev [b], N. Khaustova [a], A. Tikhonova [e], O. Gustafsson [f], T. Tesi [g], J. Martens [f], M. Jakobsson [f], M. Spasennykh [a], I. Semiletov [b,c,i]

[a] *Skolkovo Institute of Science and Technology (Skoltech), Skolkovo Innovation Centre, Moscow, Russia*
[b] *V.I. Il'ichev Pacific Oceanological Institute (POI), Far East Division of the Russian Academy of Science, Vladivostok, Russia*
[c] *Higher School of Economics (HSE), Moscow, Russian Federation*
[d] *Vernadsky Institute of Geochemistry and Analytical Chemistry (GEOKhI), Russian Academy of Sciences, Moscow, Russia*
[e] *Shirshov Institute of Oceanology (SIO), Russian Academy of Sciences, Moscow, Russia*
[f] *Department of Environmental Science, Stockholm University, Stockholm, Sweden*
[g] *Istituto di Scienze Polari, Bologna, Italy*
[i] *Tomsk State University, Russia*

ARTICLE INFO

Keywords:
Eastern arctic shelf
Bottom sediments
Salinity
Temperature
Thermal property
Freezing point
Methane seep

ABSTRACT

Significant reserves of methane (CH_4) are held in the Arctic shelf, but the release of CH_4 to the overlying ocean and, subsequently, to the atmosphere has been believed to be restricted by impermeable subsea permafrost, which has sealed the upper sediment layers for thousands of years. Our studies demonstrate progressive degradation of subsea permafrost which controls the scales of CH_4 release from the sediment into the water-atmospheric system. Thus, new knowledge about the thermal state of subsea permafrost is crucial for better understanding of the permafrost -hydrate system and associated CH_4 release from the East Siberian Arctic Shelf (ESAS) – the broadest and shallowest shelf in the World Ocean, which contains about 80% of subsea permafrost and giant pools of hydrates. Meanwhile, the ESAS, still presents large knowledge gaps in many aspects, especially with respect to subsea permafrost distribution and physical properties of bottom sediments. New field data show that the ESAS has an unfrozen (ice-free) upper sediment layer, which in-situ temperature is −1.0 to −1.8 °C and 0.6°C above the freezing point. On one hand, these cold temperature patterns may be related to the presence of subsea permafrost, which currently primarily occurs in the part of the ESAS that is shallower than 100 m, while ice-bearing sediments may also exist locally under deeper water in the Laptev Sea. On the other hand, the negative bottom sediment temperatures of −1.8 °C measured on the Laptev Sea continental slope sediments underlying water columns as deep as down to 330 m may result from dissociation of gas hydrates or possibly from dense water cascading down from the shelf. In contrast, data collected on recent expeditions in the northern Laptev shelf, zones of warmer bottom temperatures are coinciding with methane seeps, likely induced by seismic and tectonic activity in the area. These warm temperatures are not seen in the East Siberian Sea area, not even in areas of methane seeps, yet with little seismic activity.

The thermal conductivity and heat capacity of bottom sediments recorded in the database of thermal parameters for the ESAS areas mainly depend on their lithification degree (density or porosity), moisture content, and particle size distribution. The thermal conductivity and heat capacity average about 1.0 W/(m·K) and 2900 kJ/(m^3·K), with ±20% and ±10% variance, respectively, in all sampled Arctic sediments to a sub-bottom interval of 0–0.5 m.

* Corresponding author. Skolkovo Institute of Science and Technology (Skoltech), Skolkovo Innovation Centre, Moscow, Russia.
E-mail address: e.chuvilin@skoltech.ru (E. Chuvilin).

https://doi.org/10.1016/j.marpetgeo.2022.105550
Received 20 October 2021; Received in revised form 13 January 2022; Accepted 13 January 2022
Available online 25 January 2022

1. Introduction

Global change is a major concern, with the Arctic attracting particular attention as here recent analyses have showed a climate warming three times faster than global average (AMAP, 2021). Considering the longer interglacial perspective, the current high standing of the sea level is holding longer than during last ~115 ka BP after the Eemian interglacial period (Behre, 1989; Mangerud, J. 1989; Pachauri and Meyer, 2014; Dutton et al., 2015; Masson-Delmotte et al., 2021). The progressive thawing of the subsea permafrost has been connected to large-scale methane emissions into the Russian Arctic Seas (Shakhova et al. 2010a, 2010b; 2015, 2017, 2019). Significant reserves of CH_4 are held in the Arctic seabed (Soloviev et al., 1987; Kvenvolden, 1988), but the release of CH_4 to the overlying ocean and, subsequently, to the atmosphere has been believed to be restricted by impermeable subsea permafrost, which has sealed the upper sediment layers for thousands of years (Romanovskii and Hubberten, 2001). The Arctic methane emission has been the most voluminous from the East Siberian Arctic shelf (ESAS), the broadest and shallowest shelf in the World Ocean (Jakobsson, 2002), which accommodates >80% of the Earth's subsea permafrost and stores huge amounts of methane (Romanovskii and Hubberten, 2001; Shakhova et al. 2010a, 2010b; 2017). In this region, hydrate-bearing sediment deposits can reach a thickness of 400–800 m. Shallow hydrate deposits are predicted to occupy ~57% (1.25×10^6 km^2) of the East Siberian Arctic Shelf (ESAS) seabed (Soloviev, 2000). It has been suggested that destabilization of shelf Arctic hydrates could lead to large-scale enhancement of aqueous CH_4, but this process was hypothesized to be negligible on a decadal–century time scale (Kvenvolden et al., 1993; Ruppel and Kessler, 2017). However, the state of the subsea permafrost and the underlying processes of methane release and emissions remain unresolved. This constitutes one of the largest uncertainties and scientific challenges in studies of the climate system related to cryosphere-climate-carbon couplings (Gramberg et al., 1983; Romanovskii et al., 2000, 2005; Hyndman and Dallimore, 2001; Shakhova et al., 2019).

The Russian sector of the Arctic shelf is a rapidly-developed rich petroleum province (Kontorovich et al., 2010; Gulas et al., 2017). Meanwhile, the region, and specifically the ESAS, still presents large knowledge gaps in many aspects, because the harsh weather conditions, vast sea-ice coverage, and numerous related logistic problems, which make this remote region extremely hard to explore. Geological surveys, with drilling and sampling, are risky and expensive and thus remain limited (Loktev et al., 2012, 2017; Harris et al., 2018; Shakhova et al., 2017; Osterkamp and Sherman, 2019). Furthermore, the subsea permafrost may become unstable and create a potential geohazard associated with decomposition of gas hydrates, upward shifts of the gas front, and extensive methane release (Shakhova et al., 2015, 2017, 2019). The thickness of ice-rich subsea permafrost and the depth to its table have been constrained by only a modest amount of drilling and geophysical surveys, primarily in the nearshore Arctic (Shakhova et al., 2017; Koshurnikov et al., 2016), and by numerical simulations associated with much larger uncertainties than direct observations (Romanovskii et al., 2005; Nicolsky and Shakhova, 2010; Gavrilov et al., 2019). The simulation results include, for instance, the model of Shakhova et al. (2009) fitted to drilling data from the Laptev Strait and a map of subsea permafrost (Nicolsky et al., 2012) recently compiled using the 1-D Transient Heat Flux (SuPerMAP) model (Overduin et al., 2019), with reference to geothermal data collected over the 20th century from the East Siberian Arctic Shelf. The models for the ESAS region are, however, often approximate and are based on poorly reliable input data on paleoclimatic scenarios, bottom surface temperature patterns, geological models, heat flux and thermal properties of the sediments (Romanovskii and Hubberten, 2001; Romanovskii et al., 2005; Shakhova and Semiletov, 2009; Gavrilov et al., 2020). Therefore, it is an urgent need to observationally constrain the real values of input parameters, primarily, bottom sediment temperature, thermal properties, and freezing point of sediments. The published observations of temperatures, composition, and properties of the ESAS bottom sediments are geographically limited and dispersed, and only trace the most general trends and features (Grigoriev, 1966; Fartyshev, 1993; Grigoriev et al., 1996; Cheverev et al., 2007; Shakhova and Semiletov, 2007; Chuvilin et al., 2013, 2020; Russian-German cooperation system Laptev Sea: the expeditions Laptev Sea – Mamontov Klyk et al., 2011; Sergienko et al., 2012; Charkin et al., 2017; Grinko et al., 2021; Martens et al., 2021).

The Arctic shelf is an area of quite abundant seeps of methane, a major greenhouse gas, discovered as strongly elevated seawater methane levels over extensive scales across the Laptev and East Siberian Seas (Shakhova et al., 2010a; b, 2014; Lobkovsky et al., 2015) and more locally in the Barents and Kara Seas (Andreassen et al., 2017; Portnov et al., 2013; Serov et al., 2015, 2017). The seepage zones are dynamic and may in some regions be expanding (Shakhova et al., 2010a,b, 2014, 2017; Chernykh et al., 2020). The extent of methane emissions presumably depends on the stability of subsea permafrost in the eastern Arctic (Shakhova et al., 2017, 2019), but the origin of the gas remains a point of investigation (Sapart et al., 2017; Steinbach et al., 2021). On one hand, large volumes of methane may be liberated by dissociation of gas (methane) hydrates, as their stability zone is reducing in the degrading permafrost while the bottom sediments and the near-bottom water attain thermodynamic equilibrium (Archer, 2007; Shakhova and Semiletov, 2009; Chuvilin et al., 2019a,b; Shakhova et al., 2019). On the other hand, permafrost can degrade from below upwards as a result of increased heat flux. In this case, methane must be of deep origin, which is consistent with the observed correlation between the gas plumes and the zones of faulting and seismicity (Lobkovsky, 2020; Krylov et al., 2020; Steinbach et al., 2021; Bogoyavlensky et al., 2021). Numerous gas chimneys were identified in the ESAS using low frequency seismic surveys (Bogoyavlensky et al., 2021) did not reach the sediment surface, i.e. no gas flares were detected using high-resolution seismo-acoustical profiling techniques (Leifer et al., 2017; Shakhova et al., 2015, 2019). Methane was interpreted based on dual-isotopes as having a mixed biogenic and thermogenic origin (Sapart et al., 2017). A recent study using triple isotope source forensics instead pointed to a prevalence of deep-seated gas, probably thermogenic for an outer Laptev Sea seepage area (Steinbach et al., 2021). To further our understanding of the dynamics and sources of methane releasing from the subsea, it would be useful to monitor the bottom sediment temperatures near the venting sites and to compare them with the background values, in order to outline the zones of high heat flux or decomposition of gas hydrates.

The published available data on the *in-situ* seabed temperatures in the ESAS have been scanty (Shakhova and Semiletov, 2007; Loktev et al., 2012; Chuvilin et al., 2021), unlike the near-bottom water temperature measurements for other parts of the World Ocean as summarized in various databases (e.g., NOAA World Ocean Database) and maps (Vasiliev et al., 2013; Bogoyavlensky et al., 2018, 2021). The most complete hydrological database encompasses results of our research and *Roskomgidromet* monitoring, which reveals the current trend of increasing heat flux from the Lena River into the Eastern Arctic seas. The heat warms up bottom sediments, causing degradation of shallow permafrost (Shakhova and Semiletov, 2007; Shakhova et al., 2014, 2017), and increasing the area of the Lena River plume in the East Siberian Arctic shelf (Semiletov et al., 2016; Osadchiev et al., 2020). This process could be associated with the progressive permafrost thaw, increasing river discharge, and wind-driven eastward water transport (Semiletov et al., 2000). The Lena River water entering the shelf plays a principal role in warming bottom sediments; warming is distinctly pronounced in the narrow and shallow strait areas (for instance, Dmitry Laptev Strait) and adjacent shallow part of the East Siberian Sea. It has been shown that the area of its extension to the east during the first 12 years of 20th century, equal to about 116,000 km^2 (Semiletov et al., 2016).

Sub-sea permafrost is very fragile and sensitive to warming

(Romanovskii and Hubberten, 2001). Thus, a changing thermal regime over the ESAS may cause an additional increase in methane efflux into the atmosphere (Shakhova et al., 2015). Until very recently, understanding of the current thermal state and stability of the subsea permafrost–hydrate system in the ESAS was primarily based on modeling results (Romanovskii et al., 2005). Two basic mechanisms based on numerical modeling were proposed to explain permafrost dynamics after inundation: the so-called "upward degradation" under geothermal heat flux in the areas underlain by fault zones, and the so-called "downward degradation" under the warming effect of large river bodies (Shakhova et al., 2019). The latter is accelerating due to sea-ice loss and increasing warm riverine water input and contributes to warming subsea permafrost (Nicolsky and Shakhova, 2010; Shakhova and Semiletov, 2009; 2014, 2015). As a result, the thermal regime of subsea permafrost is up to 10 °C warmer than the same permafrost body remaining onshore. The near-bottom water temperature is more sensitive to seasonal air temperature variations, water column depth, offshore distance, river run-off, sea currents, etc. Than the more thermally stable bottom sediments. Therefore, equating the temperatures of near-bottom water and *in-situ* sediment temperature may be incorrect in the case of the ESAS, though such assumptions are sometimes practiced, given the data shortage.

Taken together, the lateral patterns of temperature and related physical properties of bottom sediments in the Arctic shelf, and in the continental slope of the Laptev and East Siberian Seas, require further comprehensive studies for understanding the current state of the shelf subsea permafrost. It is especially needed to constrain the bottom sediment temperatures at the sites of methane venting.

2. Study area and methods

The reported study was part of marine surveys and research expeditions in the East Siberian, Laptev and Kara Seas during the 78th and 82nd cruises of the R/V *Akademik Mstislav Keldysh* (Russia) and of the SWERUS-C3 2014 Expedition of the I/B *Oden* (Sweden) in 2014, respectively (Fig. 1), with a focus by the current study of sediments underlying seawater depths from 13 m to 541 m and revisiting mega-seeps discovered in 2011 and 2012 in the Laptev Sea (Shakhova et al., 2015).

These marine surveys revealed large methane seeps in the East Siberian and Laptev Seas (Fig. 2), with the bubbling fluxes of methane at seepage areas rising through a ~45 m thick water column and partly reaching the sea surface (Fig. 3, A). The bottom sediments were sampled at 110 sites, with a box corer, a multicorer, and a gravity corer (Fig. 3, B-D).

In-situ temperature measurements were obtained using ANTARES miniature temperature probes attached to the outside of the gravity or piston core barrel during the SWERUS-C3 Expedition. Each stainless steel temperature logger was 16 cm long and 1.5 cm in diameter. They had an operational range of −5 to 50 °C, 100 MPa, and a resolution of 0.01 °C. The probes were inserted into stainless steel fin-like fittings attached to the core barrels using large diameter hose clamps. The fins protected the temperature probes and kept them 10 cm away from the core barrel. This offset distance reduced the effects of frictional heating from the core barrel as it entered into the sediments. The probes were programmed and downloaded in the coring container before and after each deployment. During the temperature measurements, the core barrel was left in the sediments for anywhere between 1.5 and 3.5 min in order to get an accurate reading of the in-situ sediment temperature. The amount of time depended on the water depth and drift speed of the ship, which in some circumstances was >1 knot (Cruise Report SWERUS-C3, 2016a, 2016b).

During the AMK-78 and AMK-82 cruises, the temperatures of the recovered sediments were measured at ~0.3 m below the seafloor, with needle probes (100 mm in length, 3.5 mm in diameter; sensor precision 0.1 °C). The measurements were taken immediately upon sampling, after having had the probes within the sediments for 40 s to let the temperature stabilize and stay stable for 10–15 s. The temperatures measured at 10 cm from the core outer wall were assumed to represent *in situ* bottom sediment temperatures, based on the size of the cores, their thermal inertia, and rapid (5–7 min) recovery onboard (Chuvilin et al., 2021). At most of the sites, the water depths of sampling were >20 m, or below the thermocline (~15–18 m), where the water temperature was constant and likely controlled the sediment temperatures. Thus, the measured sediment temperatures at these depths are presumably constant all the year round.

We measured thermal parameters of the Arctic shelf sediments using KD-2 Pro device immediately after core recovery. KD-2 Pro is a thermal property analyzer equipped with a double needle probe and measures both thermal conductivity (λ, W/(m·K) and heat capacity (C, kJ/(m^3·K).

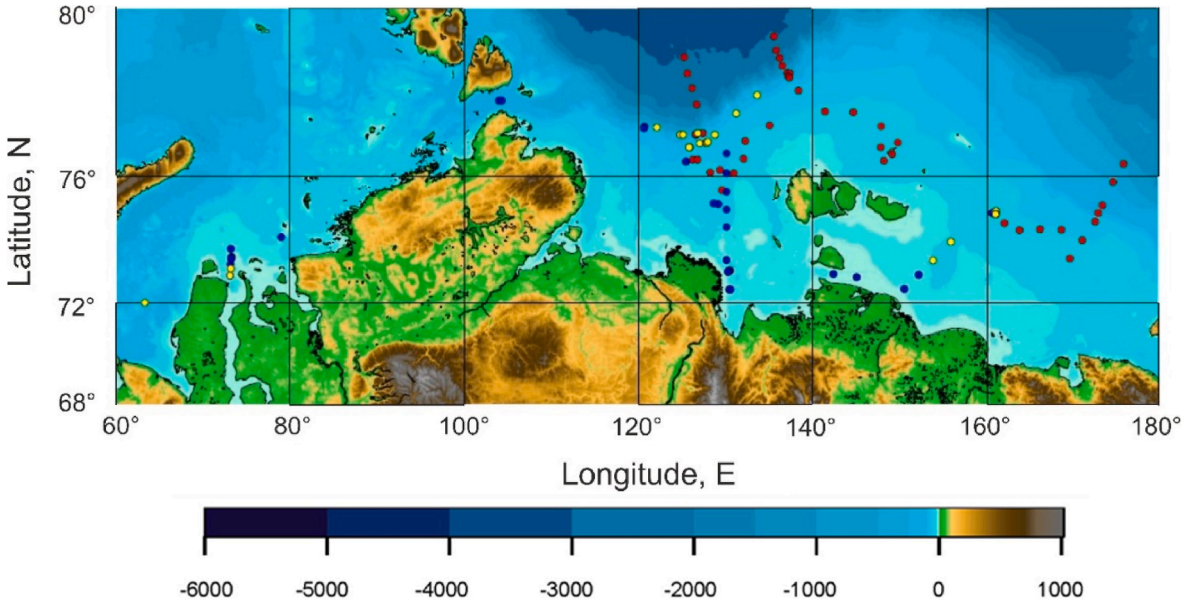

Fig. 1. Study area with the location of sampling sites in the East Siberian Sea: SWERUS-C3 cruise, 2014 (red dots); AMK-78 cruise, 2019 (yellow dots); AMK-82 cruise, 2020 (blue dots). (For interpretation of the references to colour in this figure legend, the reader is referred to the Web version of this article.)

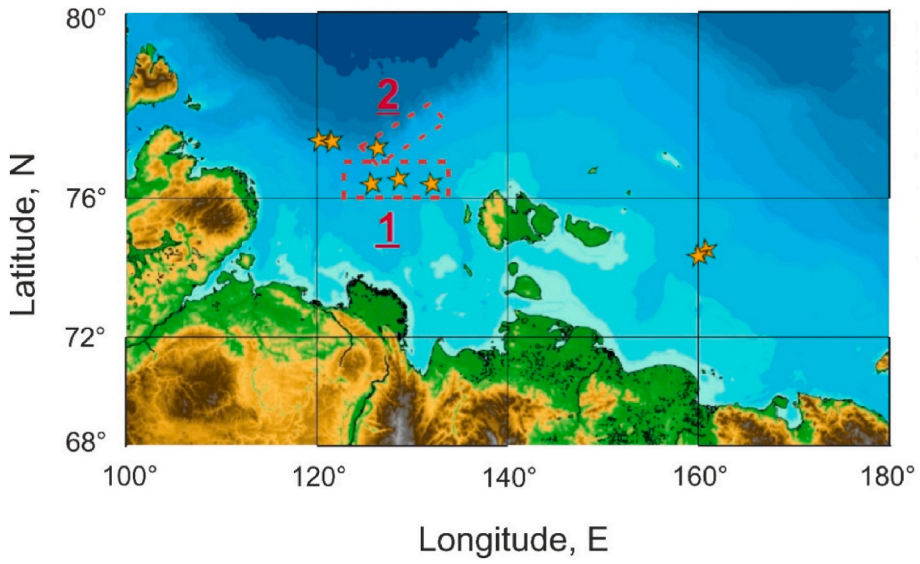

Fig. 2. Sampled zones of active seafloor methane emission in the Laptev and East Siberian seas. Orange stars mark methane seeps; red boxes frame sampling areas 1 and 2. (For interpretation of the references to colour in this figure legend, the reader is referred to the Web version of this article.)

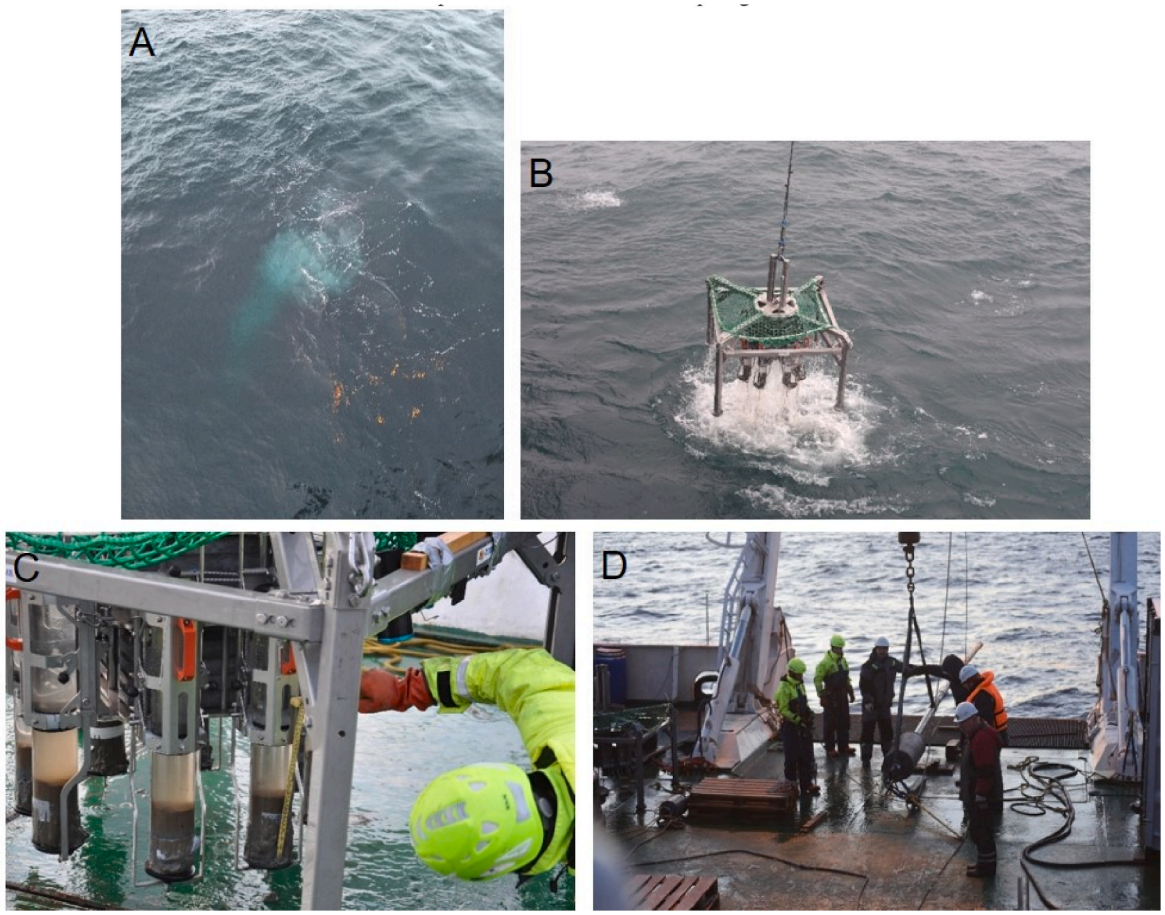

Fig. 3. Photos illustrating visual observations and sampling equipment employed during AMK-82 expedition in 2020: Panel A: bubbling methane flux rising through water in the East Siberian Sea; Panels B–C: sampling by a multicorer; and Panel D: A gravity corer.

The double probe (model SH-1) consists of two needles that are 1 cm apart. The needles have a length of 4.5 cm and a diameter of 1.2 mm, and each measurement lasts approximately 2.5 min. The thermal parameters are automatically calculated based on the results of the two cycles (heating and cooling). The accuracy of KD-2 Pro thermal conductivity and volumetric heat capacity measurements was estimated at 10% and was controlled by the standard sample equipped to the device. More detail about method and equipment is described in Chuvilin et al. (2021).

Some sediment cores were further collected for particle size distri-

bution, mineralogy, gravimetric moisture contents (W, %), bulk density (ρ, g/cm^3), dry density (ρ_d, g/cm^3), salinity (D_{sal}, %; salt-to-dry sediment weight ratio), and freezing point (T_{bf}, °C). The gravimetric moisture content W is the mass of water (M_w) per mass of dry soil (M_d), in percent:

$$W = \frac{M_w}{M_d} \times 100\% \quad (1)$$

The bulk density of bottom sediments was estimated by the cutting-ring method, using a 17 cm^3 cylinder inserted into the sediments; the cylinder and the sediments were weighed together on Ryco #820A marine scales, to an accuracy of 0.01 g.

The freezing point of the sediments was determined by the water potential method implying measurements of pore water potential (activity) and subsequent thermodynamic calculations (Istomin et al., 2017). The results agreed with direct freezing point measurements to ±0.05 °C, for different types of soil (Chuvilin et al., 2020).

The particle size distribution of the sampled bottom sediments was analyzed by combined sieving and integral suspension pressure methods (ASTM D422-63, 2007; Durner et al., 2017). The sediments were described according to the recommendations of ASTM D2487-06 (2006) and FAO Guidelines (2006). The mineralogy of the sediments was analyzed by X-ray diffractometry (XRD) on a DRON-3 analyzer (monochromatic CuKα radiation).

Stable carbon isotopes composition ($\delta^{13}C$) of methane was measured by using the isotopes ratio mass spectrometer Delta V Advantage connected to GC Isolink, including gas chromatograph Trace GC Ultra and Isolink device with combustion reactor. The gas sample (0,1–0,8 ml) was injected into the system. Gas components separation of was carried out in a CP-PoraPLOT column (27.5 m × 0.32 mm, 10 μm) with a helium as a gas-carrier. Temperature regime changed from 35°C up to 180°C with 5°C/min step. The $\delta^{13}C$ is reported in ‰ relative to VPDB standard with accuracy not more ±0.2‰.

3. Results and interpretation

The results show that the near-surface sedimentary layer over most of the East Siberian, Laptev and Kara shelf areas is composed of unfrozen (ice-free) cryotic material at negative temperatures (Table 1; Fig. 4; Appendix). The sediments are ice-free because their *in-situ* temperatures, in the presence of saline pore fluids, are at least ~0.6°C above the freezing point, which varies in the studied sediments from −1.4 to −2.3°C. The gap between in-situ temperature and the freezing point is the greatest in the continental slope of the Laptev Sea (up to 2.5°C) and in the inner shelf exposed to the effect of heat plumes from large rivers. Furthermore, the ambient temperature and estimated freezing point of bottom sediments (exclude continental slope) correlated (r^2~0.9). Warming on the shelf caused by the river plumes effect is recorded in higher freezing temperatures due to salinity decreases by dilution with fresh waters (Osadchiev et al., 2020). This effect may lead to 2–3°C warming of near-bottom water and surface sediments in the shallow-water of the East Siberian Sea shelf (Shakhova and Semiletov, 2007; Semiletov et al., 2016). Moreover, our multi-year all-season data show that in the ESAS near-shore zone the mean annual bottom water temperature has increased>0.5 °C during the (1999–2012); in summer this increase reaches>1 °C (Shakhova et al., 2014). That has been suggested that this water warming can be caused by the increasing Lena River discharge (Semiletov et al., 2000, 2016).

Table 1
Average temperatures of bottom sediments in the ESAS.

Area	Water depth (m)	Station number	Temperature[a] (°C)	Freezing point (°C)
East Siberian Sea, shelf	30–64	27	−1.3 ± 0.1[b]	−1.9 ± 0.2
East Siberian Sea, continental slope	170–468	4	+0.5 ± 0.1	–
Laptev Sea, Lena Delta	14–35	10	+0.7 ± 0.6	−1.4 ± 0.1
Laptev Sea, shelf	40–118	34	−1.3 ± 0.1	−1.9 ± 0.1
Laptev Sea, continental slope	205–541	10	+0.1 ± 0.2[c]	−2.2 ± 0.2
Kara Sea, shelf (eastern part)	20–33	5	−1.3 ± 0.1	−2.0 ± 0.2
Kara Sea, shelf (western part)	121	1	+0.3	−1.7
Vilkitsky Strait	205–230	2	−0.6	−1.8
Dmitry Laptev Strait	13–16	2	+1.7	−1.4

[a] Average temperatures for upper 0–0.5 m sediment layer.
[b] Confidence interval is calculated using on standard normal distribution with a confidence level of 0.95.
[c] Excluding stations (#15–17) with abnormal low sediment temperature (see Appendix).

The temperatures of the shallowest shelf sediments in the East Siberian Sea range from −1.1 to −1.7 °C in water depths shallower than 64 m but increase to slightly positive values (+0.4 °C) in depths deeper than 170 m (Fig. 5a). The temperatures in the Laptev Sea shelf range from +2.2 to −1.8 °C, with an average of −1.3 °C (Fig. 5b). The warmer (>0 °C) shelf sediments are restricted to the southeastern part of the Laptev Sea, which is exposed to the Lena river plume effect (Shakhova and Semiletov, 2007), while those in the central and northern sea parts are about −1.4 °C and range from −1.4 to −1.6 °C respectively. The negative bottom water temperatures in this latter area may be due to the presence of the Great Siberian flaw polynya (a zone of open water at the edge of shore ice) between the Laptev and East Siberian Seas and to descending cold waters that formed during the previous winter (Shakhova et al., 2014, 2019).

The temperature pattern of bottom sediments in the northern Laptev Sea shelf is punctuated by ~1 °C warmer spots of −0.5 to −1.0 °C (box-1 in Fig. 2). The sediment temperatures on the Laptev and East Siberian continental slopes (water depths from 200 to 541 m) range from −0.2 to +0.5 °C, most likely due to the warming effect of the near-bottom Atlantic water (Dmitrenko et al., 2010). Interestingly, the temperature of sediments on the continental slope of the Laptev Sea (box 2 in Fig. 2), in water depths deeper than 200 m, turned out to be locally below 0 °C. This could be an effect from the existence of ice-bearing subsea permafrost thicker than 350 m, which has been hypothesized based on theoretical simulations (Romanovskii and Tumskoy, 2011). However, the presence of subsea permafrost at water depths deeper than ~150 m appears unlikely because it should inevitably thaw due interaction with the >0 °C Atlantic Intermediate Water that flows along the slope (Dmitrenko et al., 2011). The low-temperature patches in the continental slope may instead result from a cooling effect of dissociation of near-bottom gas hydrates on the host and overlying sediments. Furthermore, the temperature anomalies on the continental slope may be produced by dense water cascading down from the shelf in the northwestern Laptev Sea (Ivanov and Golovin, 2007; Luneva et al., 2020). Note that relatively warm negative sediment temperatures of −0.5 to −0.6°C observed in the Vilkitsky Strait at 205–230 m sea depths confirm the previously assumed absence of modern ice-rich permafrost in that area (Gavrilov et al., 2019). The bottom sediments of the Kara Sea shelf also show negative temperatures of −1.2 to −1.4 °C, except for those affected by the Ob' River plume and those in the western sea part. The measured bottom sediment temperatures are in good agreement with previous results (Shakhova and Semiletov, 2007; Bogoyavlensky et al., 2018, 2021) and suggest the presence of buried ice-bearing permafrost in the Arctic shelf (Nicolsky et al., 2012; Gavrilov et al., 2019; Overduin et al., 2019; Matveeva et al., 2020).

The bottom sediments sampled by box corers and multicorers (core depths within 0.5 m) consist mainly of water-saturated silt loam and silt clay loam with similar mineralogy and particle sizes (Appendix). Some areas corresponding to the paleodeltas of large rivers are composed of finer-grained silty clay, while sediments in zones of active methane emission contain smaller percentages of clay particles (loam or silt loam)

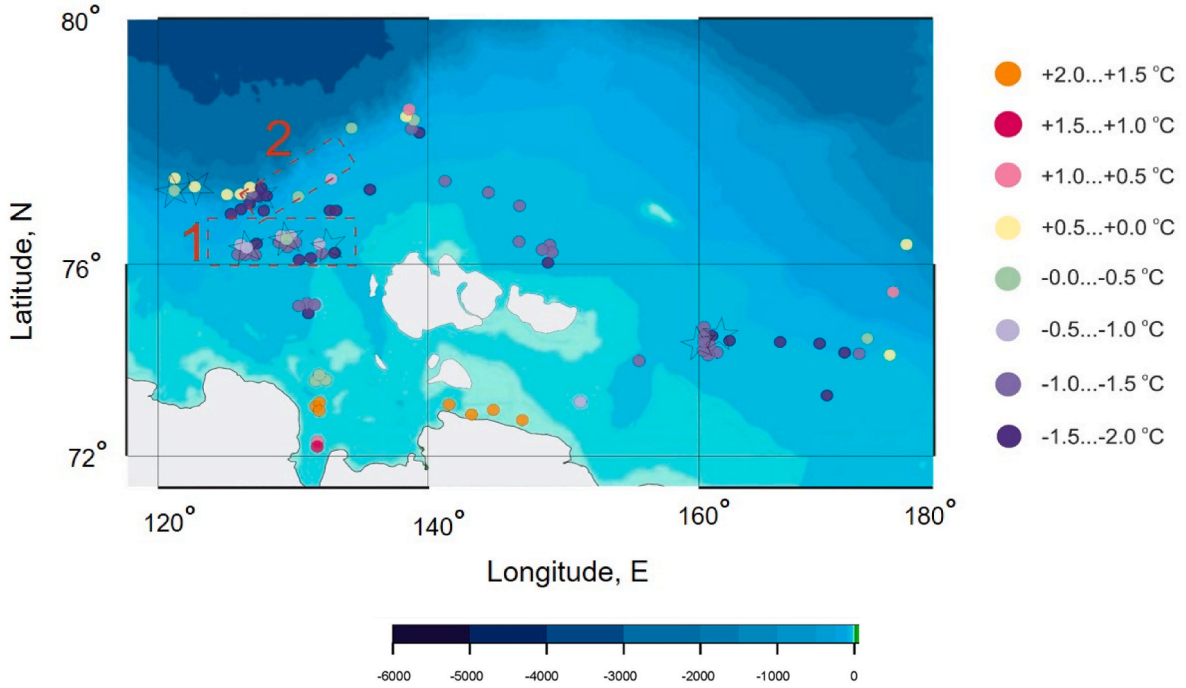

Fig. 4. Sediment temperatures in the Eastern Arctic shelves. Red boxes frame sampling areas 1 and 2 (see below). Stars mark observed methane seeps. (For interpretation of the references to colour in this figure legend, the reader is referred to the Web version of this article.)

(Table 2).

The sediments have the following properties (Appendix; Table 3): 50–80% average gravimetric moisture (80–90% in upper 10 cm); 1.5–2.5% salinity; 1.35–1.65 g/cm^3 density; ~1.53 g/cm^3 dry density; ~2.75 g/cm^3 solid density; 50–60% porosity (60–70% in upper 10 cm); thermal conductivity as low as ≤1 W/(m·K); and average heat capacity 2900 kJ/(m^3·K). The thermal conductivity variations from 0.7 to 1.3 W/(m·K) mainly correlate with the moisture content, lithification degree (density and porosity), and particle size distribution of the sediments. Thus, the average thermal conductivity and heat capacity within the 0–0.5 m depth interval are, respectively, 1.0 W/(m·K) and 2900 kJ/(m^3·K), with a variance of ±20% and ±10%.

The thermal conductivity of sediments in the region, within the interval 0.2–0.4 m sub-bottom depth, is generally higher in wetter sediments (Fig. 6), with some exceptions associated with density (porosity) and grain size heterogeneity.

The thermal conductivity of the poorly lithified Kara Sea shelf sediments (zone of the Ob' paleodelta) is less sensitive to moisture. It ranges within 0.75–0.8 W/(m·K) at a very high moisture of >100%. The thermal conductivity of the Laptev Sea sediments is more variable, ranging from 0.79 to 1.3 W/(m·K), which corresponds to a larger moisture range from 40% to 110%. The East Siberian Sea bottom sediments, with uniform grain sizes, show moderate variations both in moisture and in thermal conductivity: 65 to 54% and 0.97–1.11 W/(m·K), respectively.

The thermal conductivity within the 10–20 cm sub-bottom depths is controlled by the moisture, density, and grain size (Fig. 7) of sediments. It is in the range 0.7–1.0 W/(m·K) for the homogeneous silt and silt clay loam from the Kara Sea shelf, under 24–33 m of water; varies from 0.9 in silty clay to 1.2 W/(m·K) in loam from the East Siberian Sea sediments sampled at 16–46 m sea depths; and increases systematically from 0.9 to 1.3 W/(m·K) in the series silty clay – silt clay loam – silt loam– loam, irrespective of the sea depth in the case of the Laptev Sea shelf samples.

4. Discussion

The bottom sediments from the East Siberian, Laptev, and Kara shelf areas show similar patterns of mainly −1.4 to −1.6 °C *in situ* temperatures, which are about 0.6°C above the calculated freezing points. Thus, they are unfrozen cryotic sediments free from pore ice. These temperatures can be extrapolated to other Arctic shelf areas with similar temperature regimes, except for the zones affected by the large Siberian rivers. Ice-rich subsea permafrost may be widespread in the territory from the East Siberian shelf to the continental slope ~1000 km offshore, and it may occur locally on the Laptev Sea continental slope at >200 m water depths, where its thickness may exceed 350 m, unlike the continental slope of the East Siberian Sea. The existence of 400–500 m thick ice-rich permafrost at outer Laptev Sea shelf was hypothesized by Romanovskii and Tumskoy (2011) based on a retrospective review of the Arctic permafrost evolution. However, the lack of even implicit evidence has led to conclusion that there are no buried ice-bearing sediments below 120 m water depth in the Laptev Sea, nor elsewhere in the Eastern Arctic shelf (Loktev et al., 2012; Overduin et al., 2019; Matveeva et al., 2020; Bogoyavlensky et al., 2021). The few zones of −1.4 to −1.8 °C bottom sediment temperatures discovered locally along the Laptev Sea continental slope may instead result from a cooling effect of dissociating submarine gas hydrates or from dense water cascading down-slope. Additional marine seismic and hydrological surveys are required to elucidate the true origin of these cryotic zones.

Field data from the northern Laptev shelf in water depths between 64 and 73 m reveal temperature patches that are ~1 °C warmer than in the surrounding areas: −0.5 to −1.1 °C versus −1.4 to −1.6 °C. The zones of warmer bottom sediments spatially coincide with large methane seeps reported many times from this part of the Laptev Sea (Shakhova et al., 2010a, 2014, 2019; Chernykh et al., 2020; Steinbach et al., 2021). The temperature anomalies are apparently associated with zones of relatively high heat flux along basement faults. According to experimental evidence (Chuvilin et al., 2016), about 1 °C warming of permafrost (from −1.5 °C to −0.5 °C) may be enough for pore ice to melt and thus to make the sediments about two orders of magnitude more permeable to gas. Thus, local warming of subsea permafrost from below produces favorable conditions for methane venting into the water through permeable conduits. Unlike the zone of methane seepage in the Laptev shelf, no thermal anomalies have been found in such zones of the East Siberian shelf (~45 m water depth), though the gas phase in the two

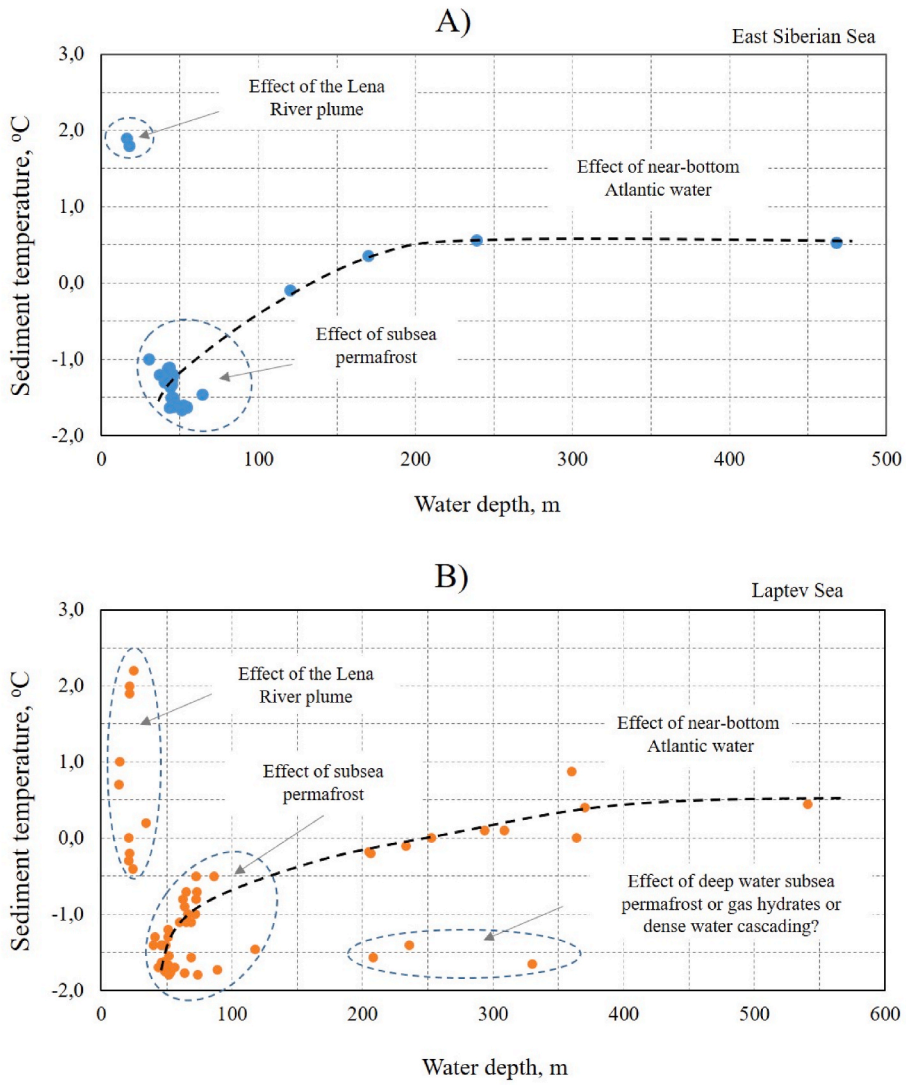

Fig. 5. Sediment temperatures vs. water depths for the East Siberian (A) and Laptev (B) seas.

shelf areas has similar components (predominant methane) and carbon isotope compositions ($\delta^{13}C$ from −59.6 to −56.7‰ VPDB), and thus may be of the same origin. However, the obtained results fail to provide reliable constraints on the gas origin. It may be either deep gas from petroleum reservoirs or sub- and intra-permafrost gas released from dissociated hydrates. Prominent temperature anomalies may be lacking from the zones of methane seepage in the East Siberian shelf because the seeps are younger (and hence smaller and fewer) than those of the Laptev shelf and thus have not yet carved through the thick subsea permafrost.

The synthesis of all data on the thermal properties of bottom sediments in the Arctic shelf shows variance reaching ±20% for thermal conductivity and ±10% for heat capacity, depending on moisture content, density (porosity), and particle size distribution. For instance, thermal conductivity is the highest (1.34–1.27 W/(m·K)) in samples with largest percentages of sand-size particles from the Laptev Sea continental slope and the lowest (0.70–0.74 W/(m·K)) in soft silty clay from the Ob' paleodelta in the Kara Sea. Furthermore, thermal conductivity shows a decreasing trend correlated with increasing gravimetric moisture in all sampled bottom sediments, though does not change much and averages about 0.8 W/(m·K) at moisture exceeding 110%. Thus, all available data indicate that the average thermal conductivity and heat capacity of bottom sediments in the Arctic shelf, within 0–0.5 m sub-bottom depth, are about 1.0 W/(m·K) and 2900 kJ/(m^3·K), respectively. The obtained results correlate well with earlier data (Cruise Report SWERUS-C3, 2016a, 2016b; Stranne et al., 2016, 2017; Chuvilin et al., 2013, 2021), where average values of thermal conductivity and heat capacity of seabed (up to 0–1 m depth) ESAS sediments varied in the intervals 0.84–1.09 W/(m·K) and 2841–3319 kJ/(m^3·K), respectively.

5. Conclusions

The data presented confirm that the East Siberian, Laptev and Kara shelves have unfrozen (ice-free) cryotic sediments on the top, with −1.0 to −1.8 °C negative temperatures, i.e. 0.6 °C above the freezing point. The shallow bottom sediments apparently lie over buried ice-rich permafrost, which is however absent or deepened in the shallow shelf waters impacted by the river heating effect and at water depths >100 m, where the sediment temperatures are above 0 °C. However, some local zones of permafrost may exist also at deeper depths of the Laptev Sea.

Surveys in the northern Laptev Sea shelf have revealed patches of warmer bottom sediments spatially associated with methane seeps. The temperature anomalies in these areas are most likely produced by a

Table 2
Properties of sediment samples.

Sampling site *(# station)*	Water depth, m	Particle size distribution, %							Moisture content, wt %	Solid density, g/cm^3	Salinity (D_{sal}), %	Total organic carbon (TOC) content[a], wt %	Plasticity index, %	Plastic limit, %	Liquid limit, %	Description according to Guidelines FAO 2006	Description according to ASTM D2487-06
		>0.5	0.5–0.25	0.25–0.1	0.1–0.05	0.05–0.01	0.01–0.002	<0.002									
Kara Sea, eastern part, Yenisei Bay *(7006)*	33.0	–	1.0	3.2	4.4	23.4	27.6	40.4	124.4	2.80	3.58	7.0	16.7	32.2	48.9	Silty clay	Lean clay with sand
Laptev Sea shelf, central area *(6984)*	49.5	–	0.1	6.5	2.2	20.0	40.6	30.6	77.3	2.69	2.48	5.8	18.5	26.4	44.9	Silt clay loam	Lean clay with sand
Laptev Sea shelf, northern area *(6516)*	66.5	–	0.1	13.5	1.1	24.0	29.3	32.0	82.4	2.75	2.69	5.3	18.9	22.5	41.4	Silt clay loam	Lean clay with sand
Laptev Sea shelf, northern area, seep area *(6948)*	72.5	–	0.7	35.4	9.5	13.6	22.1	18.7	49.4	2.74	1.49	2.8	11.9	14.8	26.7	Loam	Lean clay with sand
Laptev Sea Shelf, continental slope *(6960)*	206.5	–	–	2.1	2.3	19.1	33.5	43.0	62.9	2.76	2.02	4.8	19.5	19.9	39.4	Silty clay	Lean clay with sand
Laptev Sea Shelf, continental slope, 0–15 cm depth *(6939)*	293.5	0,5	1.0	8.5	3.8	17.7	48.6	19.9	37.7	2.79	1.74	5.1	13.4	21.1	34.5	Silt loam	Lean clay with sand
Laptev Sea Shelf, continental slope, 64–79 cm depth *(6939)*	293.5	1,4	1.7	1.9	6.3	20.8	55.4	12.5	45.1	2.78	1.42	4.9	16.2	21.6	37.8	Silt loam	Lean clay with sand
Laptev Sea Shelf, continental slope *(6527)*	370.0	–	0.1	0.4	3.1	32.3	36.1	28.0	61.5	2.80	2.50	4.8	21.7	29.3	51.0	Silt loam	Fat clay with sand
East Siberian Sea shelf *(6967)*	30.0	–	–	0.5	3.2	32.1	38.5	25.7	68.4	2.75	1.86	4.4	15.1	21.7	36.8	Silt loam	Lean clay with sand
East Siberian Sea shelf, Benetta Island area *(6468)*	37.0	–	–	0.6	9.2	45.1	18.0	27.1	53.7	2.70	1.77	4.3	25.9	20.8	46.7	Silt clay loam	Lean clay with sand
East Siberian Sea shelf, *(6476)*	46.0	–	0.1	1.1	14.8	20.5	34.0	29.5	52.7	2.74	1.58	4.0	13.5	19.9	33.4	Silt clay loam	Lean clay with sand

[a] TOC content determinates by loss on ignition at 525°C during 4 h and calculates as organic matter-to-dry sediment weight ratio.

Table 3
Thermal properties of bottom sediments on the Eastern Arctic shelf (interval 0–0.5 m below the seabed).

Area	Sea depth, m	λ, W/(m·K)	C, kJ/(m^3·K)
East Siberian Sea, shelf	30–48	1.07 ± 0.05	2768 ± 65
Laptev Sea, southern part	14–25	1.01 ± 0.10	2861 ± 80
Laptev Sea, central and northern part	25–87	1.00 ± 0.05	2842 ± 65
Laptev Sea, continental slope	206–370	1.03 ± 0.11	2906 ± 195
Kara Sea	20–33	0.84 ± 0.06	3076 ± 80

relatively high heat flux from deformed crust along basement faults. Local warming of permafrost from below became favorable for methane venting into the water through permeable zones. Unlike the Laptev Sea shelf, the zones of methane seepage in the East Siberian shelf are free from temperature anomalies, though the gas emitted in the two areas is compositionally similar (predominant methane with −59.6 to −56.7‰ δ^{13}C VPDB) and thus may have the same origin. The absence of warmer sediments in the zones of methane emission in the East Siberian shelf can be explained by a greater thickness of subsea permafrost and younger ages of the seeps. The activity of the younger seeps may have been too short to melt out permeable gas conduits of sufficient sizes and numbers, whereas the older seeps in the Laptev Sea have produced large permeable zones detectable by bottom sediment sampling.

The thermal properties of bottom sediments in the Arctic shelf are controlled by their moisture content, density, and particle size distribution. Namely, thermal conductivity reaches 1.34 W/(m·K)) in samples with largest percentages of sand-size particles from the Laptev Sea continental slope but is as low as 0.72 W/(m·K)) in soft silty clay from the Ob' paleodelta in the Kara Sea. In general, the variations are ±20% for thermal conductivity and ±10% for heat capacity of bottom sediments within 0.5 m subbottom depth. The obtained average values of 1.0 W/(m·K) and 2900 kJ/(m^3·K), respectively, can be used for reference in most of practical applications.

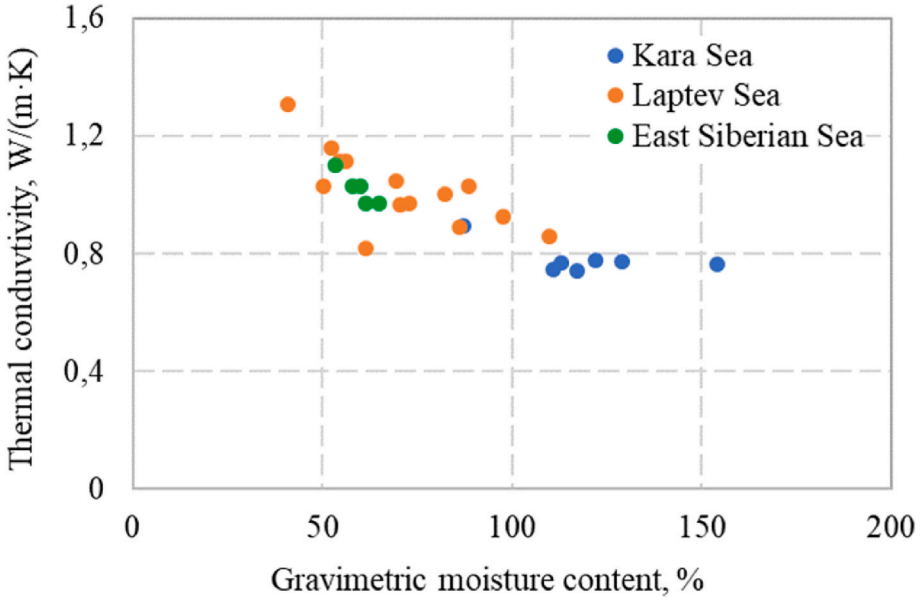

Fig. 6. Thermal conductivity vs. gravimetric moisture of bottom sediments (within the interval 0.2–0.4 m) in the Arctic shelf.

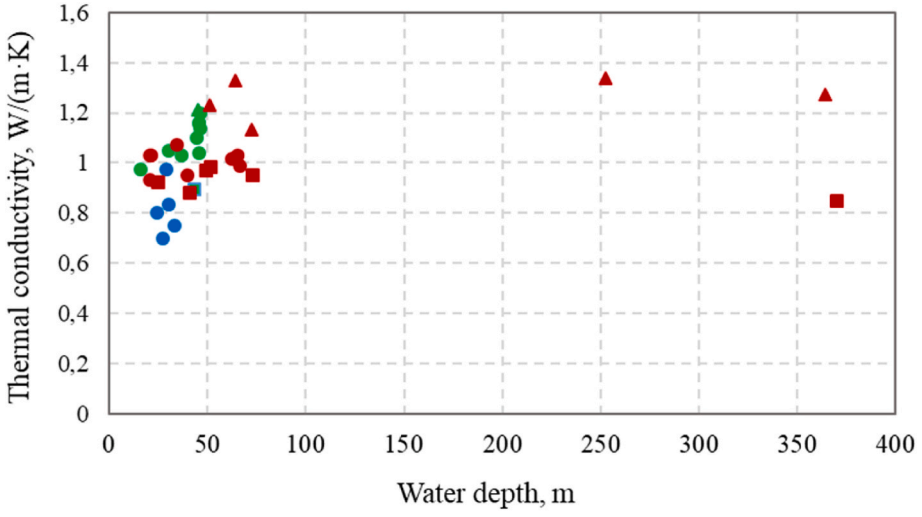

Fig. 7. Thermal conductivity of different sediments' particle sizes (core depth 10–20 cm) vs sea depth. The samples are from the East Siberian (green), Laptev (red), and Kara (blue) seas. Circles, triangles, and squares mark, respectively, silty clay and silt clay loam, loam, and silt loam. (For interpretation of the references to colour in this figure legend, the reader is referred to the Web version of this article.)

Credit author statement

Evgeny Chuvilin: Conceptualization, Methodology, Data analysis, Writing - original draft, Writing - review & editing. **Boris Bukhanov**: Conceptualization, Supervision, Methodology, Field Investigations, Laboratory Investigations, Data analysis, Visualization, Writing - original draft, Writing - review & editing. **Anna Yurchenko**: Field Investigations, Laboratory Investigations. **Dinara Davletshina**: Laboratory Investigations, Visualization. **Natalia Shakhova**: Data analysis, Writing - original draft, Writing - review & editing. **Eduard Spivak**: Field Investigations, Visualization. **Valery Rusakov**: Field Investigations, Data analysis, Writing - review & editing. **Oleg Dudarev**: Field Investigations, Supervision. **Nadezhda Khaustova**: Field Investigations, Data analysis. **Anna Tikhonova**: Field Investigations, Data analysis. **Örjan Gustafsson**: Methodology, Supervision, Field Investigations, Data analysis, Writing - review & editing. **Tommaso Tesi**: Field Investigations, Data analysis, Writing - review & editing. **Jannik Martens**: Field Investigations, Writing - review & editing. **Martin Jakobsson**: Supervision, Field Investigations, Writing - review & editing. **Mikhail Spasennykh**: Supervision, Methodology, Writing - review & editing. **Igor Semiletov**: Field Investigations, Data analysis, Writing - original draft, Writing - review & editing.

Declaration of competing interest

The authors declare that they have no known competing financial interests or personal relationships that could have appeared to influence the work reported in this paper.

Acknowledgments

This field-based study was supported by the Russian Science Foundation, RSF (grant: 21-77-30001), the European Research Council (ERC Advanced Grant CC-TOP 695331) and the Swedish Research Council (grant 2017–01601). Lab investigations were supported by the RSF (grants: 21-77-10074, 18-77-10063). The authors are grateful to the Skolkovo Institute of Science and Technology, and the Ministry of Science and Higher Education of the Russian Federation (grant 075-15-2020-928 to HSE, grant 121021500057–4 to POI, grant 0128-2021-0006 to SOI) for overall support. The Skoltech's authors are grateful to the Fablab and Machine Shop (Skoltech) for design and production cutting-ring set for sediment sampling.

Appendix A. Supplementary data

Supplementary data to this article can be found online at https://doi.org/10.1016/j.marpetgeo.2022.105550.

References

Amap, 2021. Arctic Climate Change Update 2021: Key Trends and Impacts. Summary for Policy-Makers. Arctic Monitoring and Assessment Programme (AMAP), Tromsø, Norway, p. 16. https://www.amap.no/documents/doc/arctic-climate-change-update-2021-key-trends-and-impacts.-summary-for-policy-makers/3508.

Andreassen, K., Hubbard, A., Winsborrow, M., Patton, H., Vadakkepuliyambatta, S., Plaza-Faverola, A., Gudlaugsson, E., Serov, P., Deryabin, A., Mattingsdal, R., Mienert, J., Bunz, S., 2017. Massive blow-out craters formed by hydrate-controlled methane expulsion from the Arctic seafloor. Science 356, 948–953. https://doi.org/10.1126/science.aal4500.

Archer, D., 2007. Methane hydrate stability and anthropogenic climate change. Biogeosciences 4, 521–544. www.biogeosciences.net/4/521/2007/.

ASTM D 2487 – 06, 2006. Standard Practice for Classification of Soils for Engineering Purposes (Unified Soil Classification System). Annual Book of ASTM Standards.

ASTM D422–63, 2007. Standard Test Method for Particle-Size Analysis of Soils. Annual Book of ASTM Standards.

Behre, K.E., 1989. Biostratigraphy of the last glacial period in Europe. Quat. Sci. Rev. 8, 25–44. https://doi.org/10.1016/0277-3791(89)90019-X.

Bogoyavlensky, V., Kishankov, A., Yanchevskaya, A., Bogoyavlensky, I., 2018. Forecast of gas hydrates distribution zones in the Arctic Ocean and adjacent shore Areas. Geosciences 8, 453. https://doi.org/10.3390/geosciences8120453.

Bogoyavlensky, V.I., Kazanin, A.G., Kishankov, A.V., Kazanin, G.A., 2021. Earth degassing in the Arctic: comprehensive analysis of factors of powerful gas emission in the Laptev Sea. Arctic: Ecol. Econ. 2 (2021), 178–194. https://doi.org/10.25283/2223-4594-2021-2-178-194 (in Russian).

Charkin, A.N., van der Loeff, M.R., Shakhova, N.E., Gustafsson, Ö., Dudarev, O.V., Cherepnev, M.S., Salyuk, A.N., Koshurnikov, A.V., Spivak, E.A., Gunar, A.Yu, Semiletov, I.P., 2017. Discovery and characterization of submarine groundwater discharge in the Siberian Arctic seas: a case study in Buor-Khaya Gulf, Laptev Sea. Cryosphere 11, 2305–2327. https://doi.org/10.5194/tc-11-2305-2017.

Chernykh, D., Yusupov, V., Salomatin, A., Shakhova, N., Gershelis, E., Konstantinov, A., Grinko, A., Chuvilin, E., Dudarev, O., Koshurnikov, A., Semiletov, I., 2020. Sonar estimation of methane bubble flux from thawing subsea permafrost: a case study from the Laptev sea shelf. Geosciences 10, 411. https://doi.org/10.3390/geosciences10100411.

Cheverev, V.G., Vidyapin, I.Yu, Tumskoy, V.E., 2007. Composition and characteristics of the thermokarst lagoon deposits, Bykovsky peninsula. Kriosfera Zemli 11 (3), 44–50.

Chuvilin, E.M., Bukhanov, B.A., Tumskoy, V.E., Shakhova, N.E., Dudarev, O.V., Semiletov, I.P., 2013. Thermal conductivity of bottom sediments in the region of Buor-Khaya Bay (shelf of the Laptev Sea). Kriosfera Zemli 17 (2), 32–40.

Chuvilin, E.M., Grebenkin, S.I., Sacleux, M., 2016. Influence of moisture content on permeability of sandy soils in frozen and unfrozen states. Earths Cryosphere 20 (3), 71–78.

Chuvilin, E., Ekimova, V., Bukhanov, B., Grebenkin, S., Shakhova, N., Semiletov, I., 2019a. Role of salt migration in destabilization of intra permafrost hydrates in the Arctic Shelf: experimental modeling. Geosciences 9, 188. https://doi.org/10.3390/geosciences9040188.

Chuvilin, E., Davletshina, D., Ekimova, V., Bukhanov, B., Shakhova, N., Semiletov, I., 2019b. Role of warming in destabilization of intrapermafrost gas hydrates in the Arctic Shelf: experimental modeling. Geosciences 9, 407. https://doi.org/10.3390/geosciences9100407.

Chuvilin, E.M., Sokolova, N.S., Bukhanov, B.A., Istomin, V.A., Mingareeva, G.R., 2020. The water potential method for determination of the freezing point of soils. Earths Cryosphere 24 (6), 11–20.

Chuvilin, E., Bukhanov, B., Grebenkin, S., Tumskoy, V., Shakhova, N., Dudarev, O., Semiletov, I., Spasennykh, M., 2021. Thermal properties of sediments in the east Siberian Arctic seas: a case study in the Buor-Khaya Bay. Mar. Petrol. Geol. 123, 104672. https://doi.org/10.1016/j.marpetgeo.2020.104672.

Cruise Report SWERUS-C3. Leg 1., 2016. SU-AB, Stockholm, ISBN 978-91-87355-20-2.

Cruise Report SWERUS-C3. Leg 2, 2016. SU-AB, Stockholm, ISBN 978-91-87355-21-9.

Dmitrenko, I.A., Ivanov, V.V., Kirillov, S.A., Vinogradova, E.L., Torres-Valdés, S., Bauch, D., 2011. Properties of the Atlantic derived halocline waters over the Laptev Sea continental margin: evidence from 2002 to 2009. J. Geophys. Res. 116, 1–9. https://doi.org/10.1029/2011JC007269.

Dmitrenko, I.A., Kirillov, S.A., Tremblay, L.B., Bauch, D., Hölemann, J.A., Krumpen, T., Kassens, H., Wegner, C., Heinemann, G., Schröder, D., 2010. Impact of the Arctic ocean Atlantic water layer on Siberian shelf hydrography. J. Geophys. Res. 115, C08010. https://doi.org/10.1029/2009JC006020.

Dutton, A., Carlson, A.E., Long, A.J., Milne, G.A., Clark, P.U., Deconto, R., Horton, B.P., Rahmstorf, S., Raymo, 2015. Sea-level rise due to polar ice-sheet mass loss during past warm periods. Science 349 (6244). https://doi.org/10.1126/science.aaa4019.

Durner, W., Iden, S.C., von Unold, G., 2017. The integral suspension pressure method (ISP) for precise particle-size analysis by gravitational sedimentation. Water Resour. Res. 53, 33–48. https://doi.org/10.1002/2016WR019830.

Fartyshev, A.I., 1993. Features of Offshore Permafrost in the Laptev Sea Shelf. Nauka, Novosibirsk (in Russian).

Gavrilov, A., Pavlov, V., Fridenberg, A., Boldyrev, M., Khilimonyuk, V., Pizhankova, E., Buldovich, S., Kosevich, N., Alyautdinov, A., Ogienko, M., Roslyakov, A., Cherbunina, M., Ospennikov, E., 2019. The current state and 125kyrhistory of permafrost in the Kara Sea Shelf :Modeling constraints. Cryosphere 14, 1857–1873 https ://doi.org/10.5194/tc-2019-112.

Gavrilov, A., Malakhova, V., Pizhankova, E., Popova, A., 2020. Permafrost and gas hydrate stability zone of the glacial part of the East-Siberian shelf. Geosciences 10 (484), 97. https://doi.org/10.3390/geosciences10120484Guidelines for Soil Description, 4th edition. 2006. FAO, Rome,.

Gramberg, I.S., Kulakov, Yu N., Pogrebitsky, YuE., Sorokov, D.S., 1983. Arctic oil and gas super basin. In: Proc. 11th World Petroleum Congress, London, pp. 93–99.

Grigoriev, N.F., 1966. Permafrost in the Yakutian Coastal Zone. Nauka, Moscow (in Russian).

Grigoriev, M.N., Imaev, V.S., Imaev, L.P., Koz'min, B.M., Kunitskiy, V.V., Mikulenko, K. I., Skriabin, R.M., Timirshin, K.V., 1996. Geological, Seismic and Cryogenic Processes in the Arctic Region of West Yakutia. Yakutian Science Center, Yakutsk (in Russian).

Grinko, A.A., Goncharov, I.V., Oblasov, N.V., Gershelis, E.V., Shaldybin, M.V., Shakhova, N.E., Zarubin, A.G., Ruban, A.S., Dudarev, O.V., Veklich, M.A., Mazurov, A.K., Semiletov, I.P., 2021. Characterization of organic matter of the Laptev sea eroded coastal sediments: a case study from the Cape Muostakh, Bykovsky Peninsula. Geosciences 11, 83. https://doi.org/10.3390/geosciences11020083.

Gulas, S., Downton, M., D'Souza, K., Hayden, K., Walker, T.R., 2017. Declining Arctic Ocean oil and gas developments: opportunities to improve governance and environmental pollution control. Mar. Pol. 75, 53–61. https://doi.org/10.1016/j.marpol.2016.10.014.

Harris, S.A., Brouchkov, A., Goudong, Ch, 2018. Geocryology. Characteristics and Use of Frozen Ground and Permafrost Landforms. CRC Press, Taylor & Francis Group, London, p. 765.

Hyndman, R.D., Dallimore, S.R., 2001. Natural gas hydrates studies in Canada. CSEG Rec. 5, 11–20. https://csegrecorder.com/articles/view/natural-gas-hydrate-studies-in-canada.

Istomin, V., Chuvilin, E., Bukhanov, B., Uchida, T., 2017. Pore water content in equilibrium with ice or gas hydrate in sediments. Cold Reg. Sci. Technol. 137, 60–67. https://doi.org/10.1016/j.coldregions.2017.02.005.

Ivanov, V.V., Golovin, P.N., 2007. Observations and modeling of dense water cascading from the northwestern Laptev Sea shelf. J. Geophys. Res. 112, C09003. https://doi.org/10.1029/2006JC003882.

Jakobsson, M., 2002. Hypsometry and volume of the Arctic Ocean and its constituent seas. G-cubed 3, 1–18. https://doi.org/10.1029/2001GC000302.

Kontorovich, A.E., Epov, M.I., Burshtein, L.M., Kaminskii, V.D., Kurchikov, A.R., Malyshev, N.A., Prischepa, O.M., Safronov, A.F., Stupakova, A.V., Suprunenko, O.I., 2010. Geology and hydrocarbon resources of the continental shelf in Russian Arctic seas and the prospects of their development. Russ. Geol. Geophys. 51 (1), 3–11. https://doi.org/10.1016/j.rgg.2009.12.003.

Koshurnikov, A.V., Tumskoy, V.E., Shakhova, N.E., Sergienko, V.I., Dudarev, O.V., Gunar, A.Yu, Pushkarev, P.Yu, Semiletov, I.P., Koshurnikov, A.A., 2016. The first ever application of electromagnetic soundings for mapping of submarine permafrost table on the Laptev Sea shelf. Dokl. Earth Sci. 469, 860–863. https://doi.org/10.1134/S1028334X16080110.

Krylov, A.A., Ivashchenko, A.I., Kovachev, S.A., Tsukanov, N.V., Kulikov, M.E., Medvedev, I.P., Ilinskiy, D.A., Shakhova, N.E., 2020. The seismotectonics and seismicity of the Laptev Sea region: the current situation and a first experience in a year-long installation of ocean bottom seismometers on the shelf. J. Volcanol. Seismol. 14, 379–393. https://doi.org/10.1134/S0742046320060044.

Kvenvolden, K.A., 1988. Methane hydrates and global climate. Global Biogeochem. Cycles 2, 221–229. https://doi.org/10.1029/GB002i003p00221.

Kvenvolden, K.A., Lilley, M.D., Lorenson, T.D., Barnes, P.W., McLaughlin, E., 1993. The Beaufort Sea continental shelf as a seasonal source of atmospheric methane. Geophys. Res. Lett. 20, 2459–2462. https://doi.org/10.1029/93GL02727.

Leifer, I., Chernykh, D., Shakhova, N., Semiletov, I., 2017. Sonar gas flux estimation by bubble insonification: application to methane bubble flux from seep areas in the outer Laptev Sea. Cryosphere 11, 1333–1350. https://doi.org/10.5194/tc-11-1333-2017.

Lobkovsky, L., 2020. Seismogenic-triggering mechanism of gas emission activations on the Arctic Shelf and associated phases of abrupt warming. Geosciences 11, 428. https://doi.org/10.3390/geosciences10110428.

Lobkovsky, L.I., Nikiforov, S.L., Dmitrevskiy, N.N., Libina, N.V., Semiletov, I.P., Ananiev, R.A., Meluzov, A.A., Roslyakov, A.G., 2015. Gas extraction and degradation of the submarine permafrost rocks on the Laptev Sea shelf. Oceanology 55, 283–290. https://doi.org/10.1134/S0001437015010129.

Loktev, A.S., Bondarev, V.N., Kulikov, S.I., Rokos, S.I., 2012. Russian Arctic offshore permafrost. In: Offshore Site Investigation and Geotechnics. Proc. 7th Intern. Conf., London, pp. 579–586.

Loktev, A.S., Tokarev, M.Yu, Chuvilin, E.M., 2017. Problems and technologies of offshore permafrost investigation. Procedia Eng. 189, 459–465. https://doi.org/10.1016/j.proeng.2017.05.074.

Luneva, M.V., Ivanov, V.V., Tuzov, F., Aksenov, Y., Harle, J.D., Kelly, S., Holt, J.T., 2020. Hotspots of dense water cascading in the Arctic Ocean: implications for the Pacific water pathways. J. Geophys. Res.: Oceans 125, e2020JC016044. https://doi.org/10.1029/2020JC016044.

Mangerud, J., 1989. Correlation of the Eemian and the Weichselian with deep sea oxygen isotope stratigraphy. Quat. Int. 3–4, 1–4. https://doi.org/10.1016/1040-6182(89)90067-0.

Martens, J., Romankevich, E., Semiletov, I., Wild, B., Van Dongen, B., Vonk, J., Tesi, T., Shakhova, N., Dudarev, O.V., Kosmach, D., Vetrov, A., Lobkovsky, L., Belyaev, N., Macdonald, R.W., Pienkowski, A.J., Eglinton, T.I., Haghipour, N., Dahle, S., Carroll, M.L., Astrom, E.K.L., Grebmeier, J.M., Cooper, L.W., Possnert, G., Gustafsson, O., 2021. CASCADE-the circum-Arctic sediment CArbon DatabasE. Earth Syst. Sci. Data 13, 2561–2572. https://doi.org/10.5194/essd-13-2561-2021.

Masson-Delmotte, V., Zhai, P., Pirani, A., Connors, S.L., Péan, C., Berger, S., Caud, N., Chen, Y., Goldfarb, L., Gomis, M.I., Huang, M., Leitzell, K., Lonnoy, E., Matthews, J. B.R., Maycock, T.K., Waterfield, T., Yelekçi, O., Yu, R., Zhou, B., 2021. Climate Change 2021: the Physical Science Basis. Summary for Policymakers. Contribution of Working Group I to the Sixth Assessment Report of the Intergovernmental Panel on Climate Change. IPCC. Cambridge University Press, p. 41.

Matveeva, T.V., Kaminsky, V.D., Semenova, A.A., Shchur, N.A., 2020. Factors affecting the formation and evolution of permafrost and stability zone of gas hydrates: case study of the Laptev Sea. Geoscience 12, 504. https://doi.org/10.3390/geosciences10120504.

Nicolsky, D.J., Shakhova, N.E., 2010. Modelling sub-sea permafrost in The East-siberian arctic shelf: the Dmitry Laptev Strait. Environ. Res. Lett. 5 https://doi.org/10.1088/1748-9326/5/1/015006.

Nicolsky, D.J., Romanovsky, V.E., Romanovskii, N.N., Kholodov, A.L., Shakhova, N.E., Semiletov, I.P., 2012. Modelling Sub-sea permafrost in the east Siberian Arctic shelf: the Laptev Sea region. J. Geophys. Res. 117, 429–436. https://doi.org/10.1029/2012JF002358.

Osadchiev, A.A., Pisareva, M.N., Spivak, E.A., Shchuka, S.A., Semiletov, I.P., 2020. Freshwater transport between the Kara, Laptev, and East-Siberian seas. Sci. Rep. 1, 13041. https://doi.org/10.1038/s41598-020-70096-w.

Osterkamp, T.E., Sherman, D., 2019. Sub-sea permafrost. In: Cochran, J.K., Bokuniewicz, H.J., Yager, P.L. (Eds.), Encyclopedia of Ocean Sciences, third ed. Academic Press, pp. 219–230. https://doi.org/10.1016/B978-0-12-409548-9.11574-X.

Overduin, P.P., Schneider von Deimling, T., Miesner, F., Grigoriev, M.N., Ruppel, C., Vasiliev, A., Lantuit, H., Juhls, B., Westermann, S., 2019. Submarine permafrost map in the Arctic modeled using 1-d transient heat flux (SuPerMAP). J. Geophys. Res.: Oceans 124, 3490–3507. https://doi.org/10.1029/2018JC014675.

Pachauri, R.K., Meyer, L.A. (Eds.), 2014. Climate Change 2014: Synthesis Report. Contribution of Working Groups I, II and III to the Fifth Assessment Report of the Intergovernmental Panel on Climate Change. IPCC, Geneva, Switzerland, p. 151.

Portnov, A., Smith, A.J., Mienert, J., Cherkashov, G., Rekant, P., Semenov, P., Serov, P., Vanshtein, B., 2013. Offshore permafrost decay and massive seabed methane escape in water depths >20m at the South Kara Sea shelf. Geophys. Res. Lett. 40, 3962–3967. https://doi.org/10.1002/grl.50735.

Romanovskii, N.N., Hubberten, H.-W., 2001. Results of permafrost modelling of the lowlands and shelf of the Laptev Sea region, Russia. Permafr. Periglac. Process. 12, 191–202. https://doi.org/10.1002/ppp.387.

Romanovskii, N.N., Tumskoy, V.E., 2011. Retrospective approach to the estimation of the contemporary extension and structure of the shelf cryolithozone in East Arctic. Kriosfera Zemli 15 (1), 3–14.

Romanovskii, N.N., Hubberten, H.-W., Gavrilov, A.V., Tumskoy, V.E., Tipenko, G.S., Grigoriev, M.N., Siegert, Ch, 2000. Thermokarst and land-ocean interaction, Laptev Sea region, Russia. Permafr. Periglac. Process. 11, 137–152. https://doi.org/10.1002/1099-1530(200004/06)11:2<137::AID-PPP345>3.0.CO;2-L.

Romanovskii, N.N., Hubberten, H.-W., Gavrilov, A.V., Eliseeva, A.A., Tipenko, G.S., 2005. Offshore permafrost and gas hydrate stability zone on the shelf of East Siberian seas. Geo Mar. Lett. 25, 167–182. https://doi.org/10.1007/s00367-004-0198-6.

Ruppel, C.D., Kessler, J.D., 2017. The interaction of climate change and methane hydrates. Rev. Geophys. 55, 126–168. https://doi.org/10.1002/2016RG000534.

Russian-German cooperation system Laptev Sea: the expeditions Laptev Sea – Mamontov Klyk, 2011. In: Günther, F., Overduin, P.P., Makarov, A.S., Grigoriev, M.N. (Eds.), Reports on Polar and Marine Research, 664, vol. 113. Alfred Wegener Institute for Polar and Marine Research, Bremerhaven. https://doi.org/10.2312/BzPM_0664_2013. Buor Khaya 2012, 2013.

Sapart, C.J., Shakhova, N., Semiletov, I., Jansen, J., Szidat, S., Kosmach, D., Dudarev, O., van der Veen, C., Egger, M., Sergienko, V., Salyuk, A., Tumskoy, V., Tison, J.-L., Röckmann, T., 2017. The origin of methane in the East Siberian Arctic Shelf unravelled with triple isotope analysis. Biogeosciences 14, 2283–2292. https://doi.org/10.5194/bg-14-2283-2017.

Semiletov, I.P., Savelieva, N.I., Weller, G.E., Pipko, I.I., Pugach, S.P., Gukov, A.Yu, Vasilevskaya, L.N., 2000. The dispersion of Siberian river flows into coastal waters: meteorological, hydrological, and hydrochemical aspects. In: Lewis, E.L. (Ed.), The Freshwater Budget of the Arctic Ocean, NATO Meeting/NATO ASI Series. Kluwer Academic Publishers, Dordtrecht, pp. 323–366.

Semiletov, I., Pipko, I., Gustafsson, Ö., Anderson, L.G., Sergienko, V., Pugach, S., Dudarev, O., Charkin, A., Gukov, A., Bröder, L., Andersson, A., Spivak, E., Shakhova, N., 2016. Acidification of East Siberian Arctic Shelf waters through addition of freshwater and terrestrial carbon. Nat. Geosci. 9, 361–365. https://doi.org/10.1038/ngeo2695.

Sergienko, V.I., Lobkovskii, L.I., Semiletov, I.P., Dudarev, O.V., Dmitrievskii, N.N., Shakhova, N.E., Romanovskii, N.N., Kosmach, D.A., Nikol'skii, D.N., Nikiforov, S.L., Salomatin, A.S., Anan'ev, R.A., Roslyakov, A.G., Salyuk, A.N., Karnaukh, V.V., Chernykh, D.B., Tumskoi, V.E., Yusupov, V.I., Kurilenko, A.V., Chuvilin, E.M., Bukhanov, B.A., 2012. The degradation of submarine permafrost and the destruction of hydrates on the shelf of East Arctic seas as a potential cause of the "methane catastrophe": some results of integrated studies in 2011. Dokl. Earth Sci. 446, 1132–1137. https://doi.org/10.1134/S1028334X12080144.

Serov, P., Portnov, A., Mienert, J., Semenov, P., Ilatovskaya, P., 2015. Methane release from pingo-like features across the South Kara Sea shelf, an area of thawing offshore permafrost. J. Geophys. Res. Earth Surf. 120, 1515–1529. https://doi.org/10.1002/2015JF003467.

Serov, P., Vadakkepuliyambatta, S., Mienert, J., Patton, H., Portnov, A., Silyakova, A., Panieri, G., Carroll, M.L., Carroll, J., Andreassen, K., Hubbard, A., 2017. Postglacial response of Arctic Ocean gas hydrates to climatic amelioration. Proc. Natl. Acad. Sci. U. S. A. 24, 6215–6220. https://doi.org/10.1073/pnas.1619288114.

Shakhova, N., Semiletov, I., 2007. Methane release and coastal environment in the East Siberian Arctic shelf. J. Mar. Syst. 66, 227–243. https://doi.org/10.1016/j.jmarsys.2006.06.006.

Shakhova, N.E., Semiletov, I.P., 2009. Methane hydrate feedbacks. In: Sommerkorn, M., Hassol, S.J. (Eds.), Arctic Climate Feedbacks: Global Implications. WWF International Arctic Programme, Ottawa, ISBN 978-2-88085-305-1, pp. 81–92.

Shakhova, N., Semiletov, I., Salyuk, A., Yusupov, V., Kosmach, D., Gustafsson, Ö., 2010a. Extensive methane venting to the atmosphere from sediments of the east Siberian Arctic shelf. Science 327, 1246–1250. https://doi.org/10.1126/science.1182221.

Shakhova, N., Semiletov, I., Leifer, I., Salyuk, A., Rekant, P., Kosmach, D., 2010b. Geochemical and geophysical evidence of methane release from the inner East Siberian Shelf. J. Geophys. Res. 115 https://doi.org/10.1029/2009JC005602.

Shakhova, N., Semiletov, I., Leifer, I., Sergienko, V., Salyuk, A., Kosmach, D., Chernykh, D., Stubbs, C., Nicolsky, D., Tumskoy, V., Gustafsson, Ö., 2014. Ebullition and storm-induced methane release from the east Siberian Arctic shelf. Nat. Geosci. 7 https://doi.org/10.1038/ngeo2007.

Shakhova, N., Semiletov, I., Sergienko, V., Lobkovsky, L., Yusupov, V., Salyuk, A., Salomatin, A., Chernykh, D., Kosmach, D., Panteleev, G., Nicolsky, D., Samarkin, V., Joye, S., Charkin, A., Dudarev, O., Meluzov, A., Gustafsson, Ö., 2015. The East Siberian Arctic Shelf: towards further assessment of permafrost-related methane fluxes and role of sea ice. Phil. Trans. R. Soc. A 373, 20140451 (Philosophical Transactions of the Royal Society A).

Shakhova, N., Semiletov, I., Gustafsson, O., Sergienko, V., Lobkovsky, L., Dudarev, O., Tumskoy, V., Grigoriev, M., Mazurov, A., Salyuk, A., Ananiev, R., Koshurnikov, A., Kosmach, D., Charkin, A., Dmitrevsky, N., Karnaukh, V., Gunar, A., Meluzov, A., Chernykh, D., 2017. Current rates and mechanisms of subsea permafrost degradation in the East Siberian Arctic Shelf. Nat. Commun. 8, 15872. https://doi.org/10.1038/ncomms15872.

Shakhova, N., Semiletov, I., Chuvilin, E., 2019. Understanding the permafrost–hydrate system and associated methane releases in the East Siberian Arctic Shelf. Geosciences 9, 251. https://doi.org/10.3390/geosciences9060251.

Soloviev, V.A., Ginzburg, G.D., Telepnev, E.V., Mikhaluk, YuN., 1987. Cryothermia and Gas Hydrates in the Arctic Ocean. Sevmorgeologiya, Leningrad, p. 150 (in Russian).

Soloviev, V.A., 2000. Gas-hydrate-prone areas of the ocean and gas-hydrate accumulations. In: Proceedings of the Sixth International Conference on Gas in Marine Sediments. St. Petersburg, Russia, 5–9 September 2000.

Steinbach, J., Holmstrand, H., Shcherbakova, K., Kosmach, D., Bruchert, V., Shakhova, N., Salyuk, A., Sapart, C.J., Chernykh, D., Noormets, R., Semiletov, I., Gustafsson, Ö., 2021. Source apportionment of methane escaping the subsea permafrost system in the outer Eurasian Arctic Shelf. Proc. Natl. Acad. Sci. U. S. A. 10, e2019672118 https://doi.org/10.1073/pnas.2019672118.

Stranne, C., O'Regan, M., Dickens, G.R., Crill, P., Miller, C., Preto, P., Jakobsson, M., 2016. Dynamic simulations of potential methane release from East Siberian continental slope sediments. G-cubed 17, 872–886. https://doi.org/10.1002/2015GC006119.

Stranne, C., O'Regan, M., Jakobsson, M., 2017. Modeling fracture propagation and seafloor gas release during seafloor warming-induced hydrate dissociation. Geophys. Res. Lett. 44, 8510–8519. https://doi.org/10.1002/2017GL074349.

Vasiliev, V.V., Viskunova, K.G., Kiyko, O.A., Kozlov, S.A., 2013. Geological map of the Russian federation (third generation). In: Scale 1: 1,000,000. North of Kara and Barents Seas. VSEGEI, Saint-Petersburg (in Russian).